

Optimization Problems and Algorithms from Computer Science

1	HEIKO RIEGER	
2	Theoretical Physics, Universität des Saarlandes,	
3	Saarbrücken, Germany	
4	Article Outline	
5	Glossary	
6	Definition of the Subject and its Importance	
7	Introduction	
8	Polymers in a Disordered Environment	
9	Many Repulsive Elastic Lines in Random Media	
10	Vortex Glasses and Loop Percolation	
11	Interfaces and Elastic Manifolds	
12	Random Field Ising Model	
13	The Spin Glass Problem	
14	Potts Free Energy and Submodular Functions	
15	Future Directions	
16	Bibliography	
17	Glossary	
18	Combinatorial optimization The search for an optimal	
19	configuration in terms of a cost function on a discrete	
20	set of allowed configurations.	
21	Ground state The configuration of a model for a physical	
22	system of many interacting degrees of freedom described	
23	by a Hamiltonian or energy function that has the lowest	
24	energy. Also denoted as the global minimum of the energy	
25	of the system.	
26	Disordered system A physical system with frozen in or	
27	quenched inhomogeneities, usually modeled by an energy	
28	function containing parameters that are random numbers	
29	obeying in prescribed probability distribution.	
30		
31	Universal properties Properties that do not depend on	
32	microscopic details of a physical system, like the critical	
33	exponents at a continuous phase transition or fractal	
34	dimensions.	
35	Network flows A function defined on the edges of a graph	
36	that obeys mass balance constraints at each node.	
37	A number of polynomial optimization problems relevant	
38	for disordered systems can be formulated as network	
39	flow models.	
40	Definition of the Subject and its Importance	
41	Optimization problems in statistical physics occur when-	
42	ever the ground state of a classical model for a complex	

condensed matter system has to be determined, which is necessary for understanding its low temperature properties. In some cases calculating the ground state is an easy task as for instance for the paradigmatic model for a ferromagnet: The configuration of all magnetic moments or spins with the lowest energy is the one, where all spins point in the same direction. But usually the situation is much more complex and the problem of calculating the state with the lowest energy is highly non-trivial. This occurs typically in systems with quenched disorder and/or frustration, which means that their Hamiltonian or energy function consists of competing terms that cannot be satisfied simultaneously. Powerful algorithms from computer science have been devised to find the optimum of complex cost-functions and in some cases this can even be achieved in polynomial time. In recent years many of these algorithms could be successfully applied to physically relevant model systems: to polymers in random media, interface problems in random ferromagnets, magnetic flux-lines in disordered environments, spin glasses, and many more.

Introduction

Solid materials which contain a substantial degree of quenched disorder, so called disordered systems, have been an experimental and a theoretical challenge for physicists for many decades. The different thermodynamic phases emerging in random magnets, the aging properties and memory effects of spin glasses, the disorder induced conductor-to-insulator transition in electronic or bosonic systems, the collective behavior of magnetic flux lines in amorphous high temperature superconductors, and the roughening transition of a disordered charge density wave systems are only a few examples for these fascinating phenomena that occur due to the presence of quenched disorder.

Analytic studies of models for these systems are usually based on perturbation theories valid for weak disorder, on phenomenological scaling pictures or on mean-field approximations. Therefore the demand for efficient numerical techniques that allow the investigation of the model Hamiltonians of disordered systems has always been high. Three facts make life difficult here: 1) The regime, where disorder effects are most clearly seen, are at low temperatures – and are even best visible at zero temperature; 2) the presence of disorder slows the dynamics of these systems down, they become *glassy*, such that for instance conventional Monte-Carlo or molecular dynamics simulations encounter enormous equilibration problems; 3) any numerical computation of disordered systems has to incorporate an extensive disorder average.

Please note that the pagination is not final; in the print version an entry will in general not start on a new page.

In recent years more and more model systems with quenched disorder were found that can be investigated numerically 1) at zero temperature, 2) without equilibration problems, 3) extremely fast, in polynomial time (for reviews see [1,2,3]). This is indeed progress, which became possible by the application of *exact* combinatorial optimization algorithms developed by mathematicians and computer scientists over the last few decades. This gift is not for free: first a mapping of the problem of finding the *exact* ground state of the model Hamiltonian under consideration onto a standard combinatorial optimization problem has to be found. If one is lucky, this problem falls into the class of *P*-problems, for which polynomial algorithms exist. If not, the intellectual challenge for the theoretical physicist remains to reformulate the model Hamiltonian in such a way that its universality class is not changed but a mapping on a *P*-problem becomes feasible.

An optimization problem can be described mathematically in the following way: let $\underline{\sigma} = (\sigma_1, \dots, \sigma_n)$ be a vector with n elements which can take values from a domain X^n : $\sigma_i \in X$. The domain X can be either discrete, for instance $X = \{0, 1\}$ or $X = Z$ the set of all integers (in which case it is an integer optimization problem) or X can be continuous, for instance $X = R$ the real numbers. Moreover, let \mathcal{H} be a real valued function, the cost function or objective, or in physics usually the Hamiltonian or the energy of the system. The *minimization problem* is then:

Find $\underline{\sigma} \in X^n$, which minimizes \mathcal{H} !

A maximization problem is defined in an analogous way. It is sufficient to consider only minimization problems, since maximizing a function H is equivalent to minimizing $-H$. Minimization problems in which the set X is *countable* are called *combinatorial* [4,5,6]. Optimization methods for real valued variables are treated mainly in mathematical literature and in books on numerical methods, see e. g. [8].

Constraints, must hold for the solution, may be expressed by additional equations or inequalities. An arbitrary value of $\underline{\sigma}$, which fulfills all constraints, is called *feasible*. Usually constraints can be expressed more conveniently without giving equations or inequalities. A famous example is the Traveling Salesman Problem (TSP) [7].

The TSP has attracted the interest of physicist several times. For an introduction, see [9]. The model is briefly presented here. Consider n cities distributed randomly in a plane. Without loss of generality the plane is considered to be the unit square. The minimization task is to find the shortest round-tour through all cities which visits each city only once. The tour stops at the city where it started. The

problem is described by

$$X = \{1, 2, \dots, n\} \quad (1)$$

$$H(\underline{\sigma}) = \sum_{i=1}^n d(\sigma_i, \sigma_{i+1}) \quad (2)$$

where $d(\sigma_\alpha, \sigma_\beta)$ is the distance between cities σ_α and σ_β and $\sigma_{n+1} \equiv \sigma_1$. The constraint that every city is visited only once can be realized by constraining the vector $\underline{\sigma}$ to be a permutation of the sequence $[1, 2, \dots, n]$.

The optimum order of the cities for a TSP depends on their exact positions, i. e. on the random values of the distance matrix d . It is a feature of all problems we will encounter here that they are characterized by various random parameters. Each random realization of the parameters is called an *instance* of the problem. In general, if we have a collection of optimization problems of the same (general) type, we will call each single problem an instance of the general problem.

Because the values of the random parameters are fixed for each instance of the TSP, one speaks of *frozen* or *quenched* disorder. To obtain information about the general structure of a problem one has to average measurable quantities, like the length of the shortest tour for the TSP, over the disorder.

In this article we give an overview of *methods* how to solve these problems, i. e. how to find the optimum. Interestingly, there is no single way to achieve this. For some problems it is very easy while for others it is rather hard, this refers to the time you or a computer will need at least to solve the problem, it does not say anything about the elaborateness of the algorithms which are applied. Additionally, within the class of hard or within the class of easy problems, there is no universal method. Usually, even for each kind of problem there are many different ways to obtain an optimum. Once a problem becomes large, i. e. when the number of variables n is large, it is impossible to find a minimum by hand. Then computers are used to obtain a solution. Only the rapid development in the field of computer science during the last two decades has pushed forward the application of optimization methods to many problems from science and real life.

We will review some of the most fruitful applications of polynomial algorithms from the realm of combinatorial optimization to various problems in the statistical physics of disordered systems. The next section presents the application of Dijkstra's algorithm for finding shortest paths in weighted networks to the model of a non-directed polymer in a disordered environment with isotropical correlations. Then, in the 4th and 5th section, we discuss minimum cost flow problems on weighted graphs and its solution via the

139

140

141

142

143

144

145

146

147

148

149

150

151

152

153

154

155

156

157

158

159

160

161

162

163

164

165

166

167

168

169

170

171

172

173

174

175

176

177

178

179

180

181

182

183

184

185

186

187

188 successive shortest path algorithm and apply it to the en-
 189 tanglement transition of elastic lines in a disordered envi-
 190 ronment and to the loop percolation transition in a vortex
 191 glass model. In the 6th section we focus on the minimum
 192 cut-maximum flow problem and discuss among its many
 193 applications the roughening transition of elastic media in
 194 a disordered environment. The 7th section is devoted to the
 195 random field Ising model and how its ground states can be
 196 computed with maximum-flow-minimum-cut techniques.
 197 The spin glass problem is presented in the 8th section with
 198 a mapping onto minimum weighted matching in two di-
 199 mensions and a brief outline of branch and cut methods
 200 for the higher dimensional case. The 9th section is devoted
 201 to finite temperature properties of the random bond Potts
 202 model and how its free energy can be computed in the limit
 203 of infinite Potts states. An outlook in the 10th section closes
 204 this chapter.

205 Polymers in a Disordered Environment

206 A well studied model of a single elastic line [10], like an in-
 207 dividual polymer or a single magnetic flux line in a type-II
 208 superconductor, in a disordered environment is the fol-
 209 lowing: If one excludes overhangs (and by this also self-
 210 overlaps) of the elastic lines one can parametrize its con-
 211 figuration by the longitudinal coordinate z . The line con-
 212 figuration can then be described by the transverse coordi-
 213 nate $\mathbf{r}(z)$ as a function of z . The presence of disorder is
 214 usually modeled by a random potential energy $V(\mathbf{r}, z)$ and
 215 the ground state configuration of the line is highly non-
 216 trivial due to the competition between the elastic energy,
 217 that tends to straighten the line, and the random energy,
 218 that tries to bend the line into positions of favorable energy:

$$219 \mathcal{H}_{\text{single-line}} = \mathcal{H}_{\text{elastic}} + \mathcal{H}_{\text{random}} \\ = \int_0^H dz \left\{ \frac{\gamma}{2} \left[\frac{d\mathbf{r}}{dz} \right]^2 + V[\mathbf{r}(z), z] \right\}, \quad (3)$$

220 where H is the longitudinal length (not the proper length)
 221 of the line. The random potential energy is a Gaussian
 222 variable with prescribed mean and correlations $\langle\langle V[\mathbf{r}, z]$
 223 $V[\mathbf{r}', z'] \rangle\rangle = g(\mathbf{R} - \mathbf{R}')$, where $\mathbf{R} = (\mathbf{r}, z)$ and $\langle\langle \dots \rangle\rangle$
 224 denotes the average over the disorder.

225 A lattice version of this continuum model is the *directed*
 226 polymer model: The lines correspond to directed paths on
 227 a hyper-cubic lattice that start at a specific lattice site, say
 228 $(0, 0, \dots, 0)$ and proceed only in the $(1, 1, \dots, 1)$ direction
 229 along the bonds. The energy contribution for a path passing
 230 bond \mathbf{i} of the lattice is a *positive* random variable e_i and the
 231 total energy of a path \mathcal{P} is simply

$$232 \mathcal{H}_{\text{single-line}}^{\text{lattice}} = \sum_{\mathbf{i} \in \mathcal{P}} e_i = \sum_{\mathbf{i}} e_i n_i, \quad (4)$$

233 where $n_i = 1$ if the path passes bond \mathbf{i} (i. e. $\mathbf{i} \in \mathcal{P}$) and $n_i = 0$
 234 otherwise.

235 One is interested in isotropically correlated disorder
 236 and consider the problem on a *non-directed* (square) lat-
 237 tice (i. e. paths can pass any bond in both directions) in or-
 238 der not too exclude overhangs right from the beginning. In
 239 case of uncorrelated disorder overhangs were shown to be
 240 irrelevant [12], but for isotropically correlated disorder this
 241 is not clear. The latter is defined to decay algebraically with
 242 the spatial distance of the bonds

$$243 \langle\langle e_i - e_j \rangle\rangle = |\mathbf{R}_i - \mathbf{R}_j|^{2\alpha-1}, \quad (5)$$

244 where \mathbf{R}_i spatial position of bond \mathbf{i} and α is the correla-
 245 tion exponent: Note that one expects short-range correla-
 246 tions like $\langle\langle e_i - e_j \rangle\rangle \propto \exp(-|\mathbf{R}_i - \mathbf{R}_j|/\lambda)$ with a finite
 247 correlation length λ , to be irrelevant and only long-range
 248 correlations like (5) to change the universality class of the
 249 system. Increasing α imply stronger correlations, uncorre-
 250 lated disorder corresponds to $\alpha \rightarrow -\infty$. The kind of corre-
 251 lated disorder described by (5) can be realized by generat-
 252 ing correlated random numbers are generated using a well-
 253 established numerical procedure [11].

254 Exact ground states of the Hamiltonian (4) or optimal
 255 paths are calculated using Dijkstra's algorithm (note that all
 256 energies e_i are positive). This simple polynomial algorithm
 257 works as follows: Let $V = \{1, \dots, L^d\}$ be the set of lattice
 258 sites and $A = \{(i, j) | i, j \in V \text{ nearest neighbors}\}$ the set of
 259 bonds. The algorithm increases successively a subset S of
 260 sites for which the optimal path starting at the fixed site s
 261 are known. Obviously initially $S := \{s\}$. We denote the en-
 262 ergy of the optimal path starting at s and terminating at i
 263 with $E(i)$ and since all optimal paths can be constructed via
 264 a predecessor list, we keep track of this list, too, via an array
 265 $\text{pred}(i)$, denoting the predecessor site of site i in a **shortest**
 266 **path** from s to i :

267 **algorithm** Dijkstra

268 **begin**

269 $S := \{s\}; \bar{S} := V \setminus \{s\};$

270 $E(s) := 0, \text{pred}(s) := 0;$

271 **while** $|S| < |V|$ **do**

272 **begin**

273 choose $(i, j) : E(j) := \min_{k, m} \{E(k)$

274 $+ e_{(k, m)} | k \in S, m \in \bar{S}, (k, m) \in A\};$

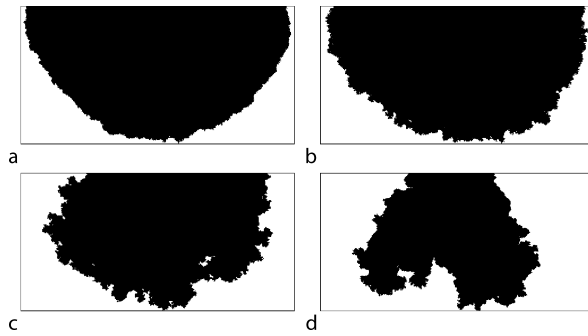
275 $\bar{S} := \bar{S} \setminus \{j\}; S := S \cup \{j\};$

276 $\text{pred}(j) := i;$

277 **end**

278 **end**

279 In Fig. 1 we show examples of the set $\{i\}$ of lattice sites that
 280 are end-points of optimal paths starting from a fixed initial



Optimization Problems and Algorithms from Computer Science, Figure 1

Example for the growth front of the non-directed polymer for uncorrelated disorder (a and b) and correlated disorder (c and d; $\alpha = 0.4$). The black pixels indicate the lattice sites of the (square) lattice are connected via optimal paths to the offspring (center of the top line) with energy less than a given value (from [13])

281 site and having a total energy $E(i)$ less than a given value
 282 E_{\max} . For uncorrelated disorder the surface of this set is
 283 roughly a semi-circle, whereas for strongly correlated dis-
 284 order the surface becomes topologically more complicated.

285 The universal properties of the optimal paths are typi-
 286 cally described the scaling of two characteristic quantities:
 287 The average transverse fluctuations $\langle\langle r^2 \rangle\rangle$ and the average
 288 energy fluctuations $\langle\langle E^2 \rangle\rangle$. Both are expected to grow al-
 289 gebraically with the the longitudinal distance H between
 290 starting point and end point of the paths:

$$291 \quad \langle\langle r^2 \rangle\rangle \propto H^\nu \quad \text{and} \quad \langle\langle E^2 \rangle\rangle \propto H^\omega, \quad (6)$$

292 where ν is called the roughness exponent and ω the energy
 293 fluctuation exponent. For uncorrelated disorder ($\alpha \rightarrow -\infty$)
 294 one knows $\nu = 2/3$ and $\omega = 1/3$. By computing the optimal
 295 paths for several thousands of samples for a given disorder
 296 correlation exponent α and for a given longitudinal dis-
 297 tances H and fitting the resulting data for transverse and
 298 energy fluctuations to the expected power laws we can ex-
 299 tract the exponents ν and ω (for details see [13]). The result-
 300 ing estimates in 2d show that the correlations are relevant
 301 for $\alpha > 0$ and the roughness exponent increases linearly for
 302 $\alpha > 0$ from its value for uncorrelated disorder $\nu = 2/3$. Al-
 303 though the number of overhangs in the optimal paths we
 304 computed in the non-directed case increased with α (i. e.
 305 increasing correlations) the fraction of bonds contributing
 306 to overhangs scaled to zero for all values of α we consid-
 307 ered. Hence overhangs appear to be irrelevant also in the
 308 presence of correlated disorder.

Many Repulsive Elastic Lines in Random Media

309

310 When one puts interacting elastic lines together into a finite
 311 system with a given density of lines they will show inter-
 312 esting collective behavior. Examples are the entanglement
 313 of magnetic flux lines in high- T_c superconductors in the
 314 mixed phase [14] or the entanglement of polymers in mat-
 315 erials like rubber [15]. The degree of entanglement of the
 316 lines usually manifests itself in various measurable prop-
 317 erties like stiffness or shear modulus in the case of poly-
 318 mers and in transport or dynamical properties for magnetic
 319 flux lines in superconductors. A theoretical description of
 320 these line systems can be based on the single-line Hamilto-
 321 nian (3) plus an appropriate line interaction term:

$$\begin{aligned} \mathcal{H}_{\text{many-lines}} = & \sum_{i=1}^N \mathcal{H}_{\text{single-line}}^{(i)} \\ & + \sum_{i < j} \int_0^L dz \int_0^L dz' V_{\text{int}}[\mathbf{R}_i(z) - \mathbf{R}_j(z')], \end{aligned} \quad (7)$$

322 where $\mathbf{R}_i(z) = (\mathbf{r}_i(z), z)$ is the spatial position of the in-
 323 finitesimal line segment dz of the i th line. If the interactions
 324 $V_{\text{int}}[\mathbf{R}_i(z) - \mathbf{R}_j(z')]$ are short ranged (i. e. in case of flux
 325 lines the screening length small compared to the average
 326 line distance) or just hard core repulsive, and the random,
 327 δ -correlated disorder potential $V_r[\mathbf{r}_i(z), z]$ in (3) is strong
 328 compared to the elastic energy ($\propto \gamma$) this continuum model
 329 reduces to a lattice model reminiscent of the single-line lat-
 330 tice model (4):
 331

$$332 \quad \mathcal{H}_{\text{many-lines}}^{\text{lattice}} = \sum_{\mathbf{i}} e_{\mathbf{i}} n_{\mathbf{i}}, \quad (8)$$

333 where $n_{\mathbf{i}} = 1$ if a line passes bond \mathbf{i} and $n_{\mathbf{i}} = 0$ otherwise
 334 and the positive random variable $e_{\mathbf{i}}$ is the energy cost for
 335 a line segment to occupy bond \mathbf{i} . The hard core constraint
 336 is thus enforced on the bonds but for the sake of an easier
 337 formal description we allow the lines to touch in isolated
 338 points, the lattice sites. The lines live on the bonds of a sim-
 339 ple cubic lattice with a lateral width L and a longitudinal
 340 height $H(L \times L \times H$ sites) with free boundary conditions in
 341 all directions. Each line starts and ends at an arbitrary po-
 342 sition on the bottom respective top planes. The number N
 343 of lines threading the sample is fixed by a prescribed den-
 344 sity $\rho = N/L^2$. For a single line $N = 1$, one recovers the non-
 345 directed polymer model (4). The random bond energies are
 346 uniformly distributed over the interval $[0, 1]$.

347 Note that the allowed configurations of the bond vari-
 348 ables $n_{\mathbf{i}}$ are only those that can be identified with lines
 349 threading the samples (or loops inside the sample, which,
 350 however, cost energy and therefore do not occur in the

ground state), which means that the number of occupied bonds connected to a lattice site that lies neither on the top nor on the bottom plane has always to be even. If we connect all sites on the top to an extra site, called the source, an all sites on the bottom to another extra site, called the target, than the latter statement remains true also for the top an bottom plane. We can now say that N lines start at the source node and terminate at the target node, or, in network flow jargon: The feasible configurations of the variables n_i constitute a flow with zero excess on all lattice sites and an excess $+N$ and $-N$ for the source and target node, respectively.

Thus the determination of the ground state configuration of the N -line problem with the Hamiltonian (8) is a **minimum-cost-flow-problem**, which can be solved with a successive shortest path algorithm [1,2,3]. In essence one starts with the zero flow $n_i = 0$, corresponding to zero lines in the system, and sends successively one unit of flow from the source to the target, corresponding to adding one line after the other to the system. This has to happen with the minimal energy, i. e. along optimal paths, which are calculated using Dijkstra's algorithm that we encountered already in the single line problem discussed in the last section. However, when trying to add a line to a system with a number, say M , of lines already present, the existing line configuration sometimes must be changed to minimize the total energy for $M + 1$ line solution. That becomes feasible by allowing flow to be sent *backwards* on already occupied bonds. By this operation one *gains* energy (whereas occupying an empty bond i always costs energy $e_i \geq 0$), which means one has to operate on a network that has to be adapted to the existing flow configuration and has negative energies on all occupied bonds. Unfortunately Dijkstra's algorithm works only for positive bond energies, and one has either to use a slower (label-correcting) algorithm to find the optimal paths in a graph with negative edge costs [3] or one has to use the concept of node potentials, by which one can make all energies in the adapted network non-negative without changing the actual shortest paths. This procedure is described in full detail in [3].

The resulting line configuration is then analyzed. One computes the winding angle of all line pairs as indicated in Fig. 2 (c.f. [16]). For each z -coordinate the vector connecting the two lines is projected onto that basal plane (*left part of Fig. 2*). $z = 0$ gives the reference line with respect to which the consecutive vectors for increasing z -coordinate have an angle $\phi(z)$. If the two lines intersect one neglects the intersection point and interpolate between the last and the next point in such a way that the global winding angle is minimized. One defines two lines to be *entangled* when $\phi(z) > 2\pi$. This choice is one that measures entanglement

from the topological perspective [17], and comes from the requirement that an entangled pair of lines can not be separated by a suitable linear transformation in the basal plane (i. e. the lines almost always would cut each other, if one were shifted). The precise definition of entanglement is not of major relevance, and the one used is useful since it is the computationally easiest.

Sets or *bundles* of pairwise entangled lines are formed so that a line belongs to a bundle if it is entangled at least with one other line in the set. The topological multi-line-entanglement could be characterized by other measures as well; the universal properties of the transition will not depend on these. These line bundles are spaghetti-like – i. e. topologically complicated and knotted sets of one-dimensional objects. To study the size distribution of these objects one projects these bundles on the basal plane, as indicated in Fig. 2, where a bundle projects onto a connected cluster. The probability for two lines to be entangled increases with increasing system height. Consequently one would expect that the bundle size increases with H , and therefore also their projections, the clusters. This scenario is exemplified in Fig. 3, for the largest height the largest cluster spans from one side of the system to the other, i. e. it *percolates*.

Hence, for a given line density ρ one expect that for system heights larger than a critical value H_c an system spanning large entangled bundle occurs, containing an infinite number of lines in the limit $L \rightarrow \infty$. One calls this an *entanglement transition* occurring at a finite system height H_c . In the projection plane this appears like a percolation transition and in [18] it was shown that this transition is in the same universality class as conventional bond percolation.

Vortex Glasses and Loop Percolation

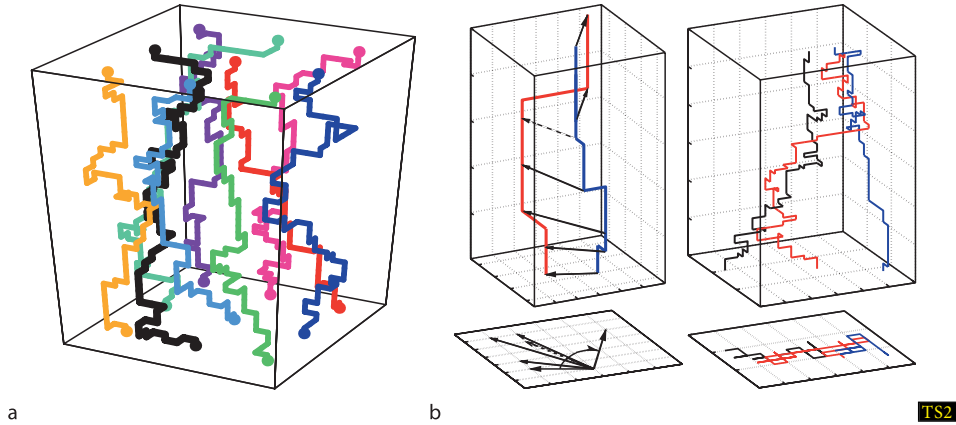
Another application of the successive shortest path algorithm for minimum-cost-flow-problems is finding the ground state of the Hamiltonian

$$H = \sum_{\mathbf{i}} (n_{\mathbf{i}} - b_{\mathbf{i}})^2 \quad (9)$$

$$\text{with the constraint } \forall k: \sum_{l \text{ n.n. of } k} n_{(kl)} = 0,$$

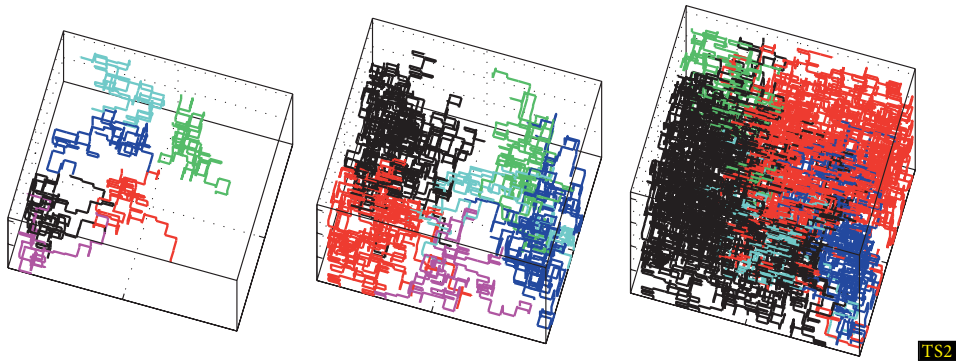
where the integer variables $n_{\mathbf{i}}$ live on the bonds \mathbf{i} of a d -dimensional hyper-cubic lattice and $b_{\mathbf{i}} \in [-2\sigma, 2\sigma]$ are real valued quenched random variables with $\sigma \geq 0$ setting the strength of the disorder. The constraint $\sum_{l \text{ n.n. of } k} n_{(kl)} = 0$ means that at all lattice sites k the incoming flow has to balance the outgoing flow, i. e. the flow $\{n_{\mathbf{i}}\}$ is divergence-less. The physical motivation of studying models these kind of models is the following:

TS2 Please note that this figure will be printed in gray in the final version.



Optimization Problems and Algorithms from Computer Science, Figure 2

Left: Ground state configuration of a N -line system with $N = 9$ defined by (8). The entry/exit points are fixed in a regular 3×3 array for better visibility. Right: Definition of the winding angle of two flux lines. Right part, top: A configuration of three lines that are entangled. Right part, bottom: The projection of the line configuration on the basal plane, defining a connected cluster



Optimization Problems and Algorithms from Computer Science, Figure 3

Line configurations for different heights H (from left to right: $H = 64, 96, 128$), the lateral size $L = 20$, the line density is $\rho = 0.3$. Only the largest line bundles are shown, indicated by a varying gray scale. Black denotes the largest cluster, which eventually percolates

447 In 2d the Hamiltonian (9) occurs for instance in the
 448 context of the solid-on-solid (SOS) model on a disordered
 449 substrate [19]. The SOS representation of a 2d surface is defined
 450 by integer height variables u_k for each lattice site k
 451 of a square lattice. The disordered substrate is modeled via
 452 random offsets $d_k \in [0, 1]$ for each lattice site, such that the
 453 total height at lattice site k is $h_k = u_k + d_k$. The the total energy
 454 of the surface is

$$455 \quad \mathcal{H}_{\text{SOS}} = \sum_{(kl)} (h_k - h_l)^2 = \sum_{(\tilde{k}\tilde{l})} (n_{(\tilde{k}\tilde{l})} - b_{(\tilde{k}\tilde{l})})^2 \quad (10)$$

456 where the first sum runs over all nearest neighbor pairs
 457 (kl) of the square lattice and the second sum runs over
 458 all bonds $(\tilde{k}\tilde{l})$ of the dual lattice (being a square lattice,
 459 too), which connect the centers of the elementary plaquettes
 460 of the original lattice. A dual bond $(\tilde{k}\tilde{l})$ therefore

crosses perpendicularly a bond (kl) connecting neighbors k 461
 and l on the original lattice. We define $n_{(\tilde{k}\tilde{l})} = n_k - n_l$ 462
 and $d_{(\tilde{k}\tilde{l})} = d_l - d_k$ if l is either the right or the upper 463
 neighbor of k (i. e. for $k = (x, y)$ either $l = (x + 1, y)$ or 464
 $l = (x, y + 1)$) and $n_{(\tilde{k}\tilde{l})} = n_l - n_k$ and $d_{(\tilde{k}\tilde{l})} = d_k - d_l$ if l is 465
 either the left or the lower neighbor of k (i. e. for $k = (x, y)$ 466
 either $l = (x - 1, y)$ or $l = (x, y - 1)$). In this way the sum 467
 over all four dual bond variables attached to one site of 468
 the dual lattice corresponds to the sum of original height 469
 variables around an elementary plaquettes in the original 470
 lattice: $(n_{(x,y)} - n_{(x,y+1)}) + (n_{(x,y+1)} - n_{(x+1,y+1)}) +$ 471
 $(n_{(x+1,y+1)} - n_{(x+1,y)}) + (n_{(x+1,y)} - n_{(x,y)}) = 0$, which 472
 implies that the flow $\{n_{(\tilde{k}\tilde{l})}\}$ is divergence free as inferred 473
 in (9). 474

In 3d the Hamiltonian (9) is the strong screening limit 475
 of the vortex glass model for disordered superconduct- 476

477 tors [20,21]

$$478 \quad \mathcal{H}_{\text{VG}} = \sum_{i,j} (n_i - b_i) G_\lambda(\mathbf{r}_i - \mathbf{r}_j) (n_j - b_j), \quad (11)$$

479 where the integer vortex variables n_i live on the bonds
480 of a simple cubic lattice and have to fulfill the constraint
481 in (9) since they represent magnetic vortex lines that are di-
482 vergence free. The real valued quenched random variables
483 $b_i \in [-2\sigma, 2\sigma]$ are derived from the lattice curl of a random
484 vector potential ($\sigma \geq 0$ being the strength of the disorder).
485 The 3d vector \mathbf{r}_i denotes the spatial positions of bond i in
486 the lattice and the sum runs over all bond pairs of the lattice
487 (not only nearest neighbors). The lattice propagator $G_\lambda(\mathbf{r})$
488 has the asymptotic form $G_\lambda(\mathbf{r}) \propto \exp(-|\mathbf{r}|/\lambda)/|\mathbf{r}|$, where λ
489 is the screening length. In the strong screening limit $\lambda \rightarrow 0$
490 only the on-site repulsion survives [20] and gets

$$491 \quad \mathcal{H}_{\text{VG}}^{\lambda \rightarrow 0} = \sum_i (n_i - b_i)^2 \quad (12)$$

492 which is the Hamiltonian (9) in 3d that we intend to discuss
493 here.

494 The ground state of (9) can again be computed with-
495 in polynomial time by a successive shortest path algo-
496 rithm [3]. As for the N -line problem one starts with a con-
497 figuration $\{n_i\}$ that optimizes the Hamiltonian in (9) but
498 does not, in general, fulfill the mass balance constraint
499 given in (9). In the N -line problem that was simply the
500 zero-flow $n_i = 0$, which does not fulfill the requirement that
501 the source and the target have excess $+N$ and $-N$, respec-
502 tively. Here we start with n_i the closest integer to the real
503 number b_i for each bond i . Since this solution violates the
504 mass-balance constraint one successively sends flow from
505 nodes that have an excess flow to nodes that have a deficit
506 along optimal paths that are again found using node poten-
507 tials (to make all costs non-negative) and Dijkstra's algo-
508 rithm. The details of this algorithm can be found in [1,2,3].

509 Figure 4 shows three typical ground state configura-
510 tions for different strength of the disorder σ in 2d and in 3d.
511 For small σ only small isolated loops occur, whereas for
512 larger σ one finds loops that extend through the whole sys-
513 tem, they percolate. A finite size scaling study of the un-
514 derlying percolation transition [22] yields a novel univer-
515 sality class with numerically estimated critical exponents
516 that differ significantly from those for conventional bond-
517 or site-percolation [22].

518 Interfaces and Elastic Manifolds

519 A system of strongly interacting (classical) particles or
520 other objects, like magnetic flux lines in a type-II supercon-
521 ductor (as we discussed in Sect. "Many Repulsive Elastic

522 Lines in Random Media" and for which the starting Hamil-
523 tonian would given by (7)), or a charge density wave system
524 in a solid, will order at low temperatures into a regular ar-
525 rangement a lattice (crystal lattice or flux line lattice). Fluc-
526 tuations either induced by thermal noise (temperature) or
527 by disorder (impurities, pinning centers) induce deviations
528 of the individual particles from their equilibrium positions.
529 As long as these fluctuations are not too strong an expan-
530 sion of the potential energy around these equilibrium con-
531 figuration might be appropriate. An expansion up to 2nd
532 order is called the elastic description or elastic approxima-
533 tion, which in a coarse grained form (where the individ-
534 ual particles that undergo displacements from their equi-
535 librium positions do not occur any more and are replaced
536 by a continuum field $\phi(\mathbf{r})$ reads then

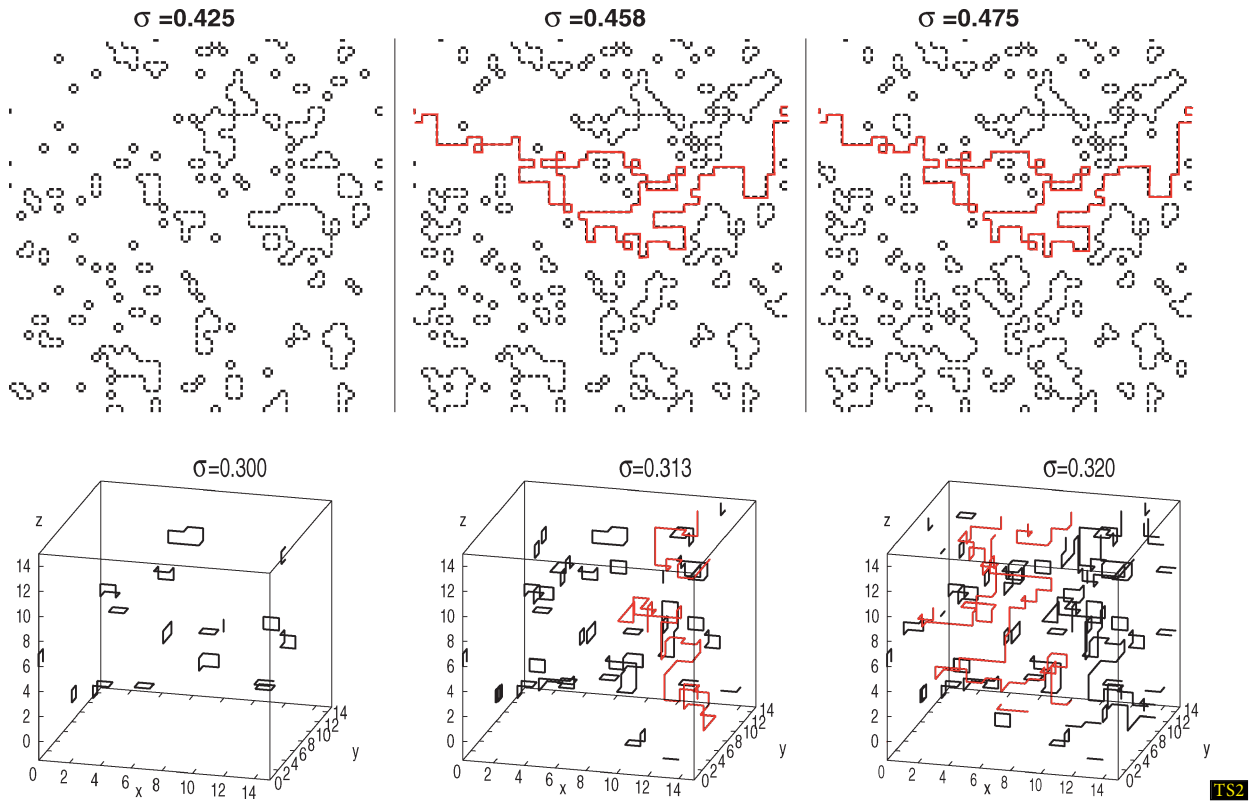
$$537 \quad \mathcal{H}_{\text{manifold}} = \mathcal{H}_{\text{elastic}} + \mathcal{H}_{\text{random}} \\ = \int d^d \mathbf{r} \left\{ \frac{\gamma}{2} |\nabla \phi(\mathbf{r})|^2 + V(\phi(\mathbf{r}), \mathbf{r}) \right\}. \quad (13)$$

538 The random potential energy is a delta-correlated Gauss-
539 ian variable with mean zero, $\langle \langle V(\phi, \mathbf{r}) V(\phi', \mathbf{r}') \rangle \rangle =$
540 $D^2 \delta(\phi - \phi') \delta(\mathbf{r} - \mathbf{r}')$. The integration extends over the
541 whole space that parameterizes the manifold, for instance
542 $d = 1$ for an elastic line in a random potential, $d = 2$ for
543 an interface or a surface in a disordered environment etc.
544 Note that for $d = 1$ one recovers the single line Hamilto-
545 nian (3). The many-line Hamiltonian (7) also allows such
546 an elastic description in the limit, in which the interactions
547 are strong and the the random potential is weak compared
548 to the elastic energy. In this limit the lines will only deviate
549 moderately from a regular, translationally invariant config-
550 uration (the Abrikosov flux line lattice). This case is called
551 an elastic periodic medium and one has to modify the ϕ -
552 part of the disorder correlator such that the Hamiltonian
553 has the correct translational symmetry [26].

554 Elastic Manifold

555 The typical example for an elastic manifold in a dis-
556 ordered environment are domain walls in the $d + 1$ di-
557 mensional random bond ferromagnet $H = -\sum_{\langle ij \rangle} J_{ij} \sigma_i \sigma_j$
558 ($J_{ij} \geq 0$, random) in which we fix all spins in the lower
559 (upper) plane, i. e. all σ_i with $i = (x_1, \dots, x_d, y)$ and $y = 1$
560 ($y = H$), to be $\sigma_i = +1(-1)$, c.f. Fig. 5. First one maps it onto
561 a flow problem in a capacitated network. One introduces
562 two extra sites, a source node s , which is connected to all
563 spins of the hyperplane $y = 1$ with bonds $J_{s, (x_1, \dots, x_d, y=1)}$
564 $= J_\infty$, and a sink node t , which is connected to all spins
565 of the hyperplane $y = H$ with bonds $J_{s, (x_1, \dots, x_d, y=H)} = J_\infty$.
566 One chooses $J_\infty = 2 \sum_{\langle ij \rangle} J_{ij}$, i. e. strong enough that the
567 interface cannot pass through a bond involving one of

TS3 Keep in mind that the figure will be printed in gray.



Optimization Problems and Algorithms from Computer Science, Figure 4

Examples of ground state configurations of the Hamiltonian (9) for varying disorder strengths σ (for particular disorder realizations). **Top:** 2d, $L = 50$, the critical disorder strength is $\sigma_c \approx 0.46$; **Bottom:** 3d, $L = 16$, the critical disorder strength is $\sigma_c \approx 0.31$. The occupied bonds ($n_i \neq 0$) are marked black, the percolating loop is marked by light gray (red) **TS2**

568 the two extra sites. Now we enforce the aforementioned
 569 boundary conditions for the spins in the upper and the
 570 lower plane by simply fixing $\sigma_s = +1$ and $\sigma_t = -1$. The
 571 graph underlying the capacitated network one has to con-
 572 sider is now defined by the set of vertices (or nodes)
 573 $N = \{1, \dots, H \cdot L^d\} \cup \{s, t\}$ and the set of edges (or arcs)
 574 connecting them $A = \{(i, j) | i, j \in N, J_{ij} > 0\}$.

575 The capacities u_{ij} of the arcs (i, j) is given by
 576 the bond strength J_{ij} . For any spin configuration $\sigma =$
 577 $(\sigma_1, \dots, \sigma_N)$ one defines $S = \{i \in N | \sigma_i = +1\}$ and $\bar{S} =$
 578 $\{i \in N | \sigma_i = -1\} = N \setminus S$. Obviously $\sigma_s \in S$ and $\sigma_t \in \bar{S}$. The
 579 knowledge of S is sufficient to determine the energy of any
 580 spin configuration via $H(S) = -C + 2 \sum_{(i,j) \in (S, \bar{S})} J_{ij}$ where
 581 $(S, \bar{S}) = \{(i, j) | i \in S, j \in \bar{S}\}$. The constant $C = \sum_{(i,j) \in A} J_{ij}$
 582 is irrelevant, i. e. independent of S . Note that (S, \bar{S}) is the set
 583 of edges (or arcs) connecting S with \bar{S} , this means it cuts N
 584 in two disjoint sets. Since $s \in S$ and $t \in \bar{S}$, this is a so called
 585 s - t -cut-set, abbreviated $[S, \bar{S}]$. Thus the problem of finding
 586 the ground state configuration of an interface in the ran-

dom bond ferromagnet can be reformulated as a **minimum**
cut problem

$$\min_{S \subset N} \{H'(S)\} = \min_{[S, \bar{S}]} \sum_{(i,j) \in (S, \bar{S})} J_{ij} \quad (14)$$

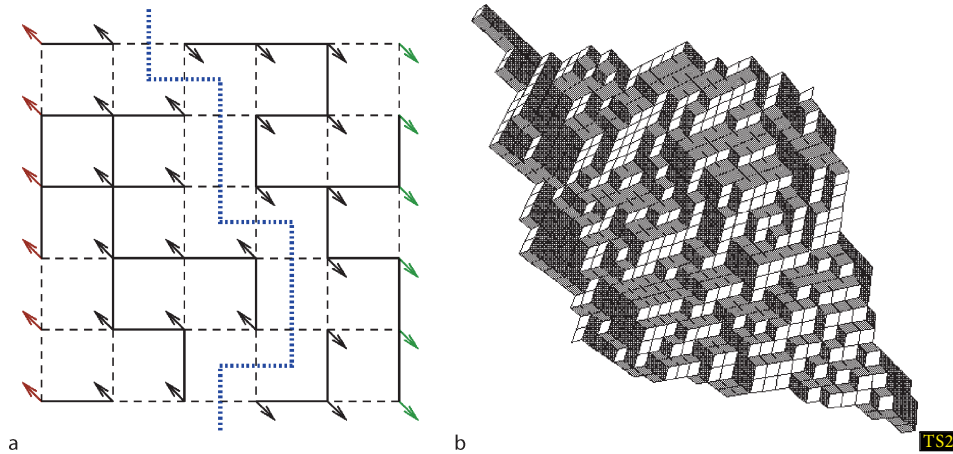
587
 588
 589 in the above defined capacitated network (with $H' = (H +$
 590 $C)/2$). It does not come as a surprise that this minimum
 591 cut is *identical* with the interface between the $(\sigma_i = +1)$ -do-
 592 main and the $(\sigma_i = -1)$ -domain that has the lowest energy.
 593 Actually any s - t -cut-set defines such an interface, some
 594 of them might consist of many components, which is of
 595 course energetically unfavorable.
 596

597 A flow in the network G is a set of nonnegative num-
 598 bers x_{ij} subject to a capacity constraint and a mass balance
 599 constraint for each arc

$$0 \leq x_{ij} \leq u_{ij}$$

$$\text{and } \sum_{\{j|(i,j) \in A\}} x_{ij} - \sum_{\{j|(j,i) \in A\}} x_{ji} = \begin{cases} -v & \text{for } i = s \\ +v & \text{for } i = t \\ 0 & \text{else} \end{cases} \quad (15)$$

587
 588
 589
 590
 591
 592
 593
 594
 595
 596
 597
 598
 599
 600



Optimization Problems and Algorithms from Computer Science, Figure 5

Left: Sketch of a 2d (RBIM) with antiperiodic boundary conditions. Broken lines represent weak bonds, full lines strong bonds, the spin configuration with the lowest energy defines an interface, as indicated, and corresponds to the minimum cut in the corresponding network flow problem. Right: An optimal interface in the 111-direction of a 3d RBIM corresponding to the ground state configuration of a 2d elastic medium with scalar displacement field (from [23])

601 This means that at each node everything that goes in has to
 602 go out, too, with the only exception being the source and
 603 the sink. What actually flows from s to t is ν , the value of
 604 the flow. The **maximum flow problem** for the capacitated
 605 network G is simply to find the flow \mathbf{x} that has the maxi-
 606 mum value ν under the constraint (15).

607 Let \mathbf{x} be a flow, ν its value and $[S, \bar{S}]$ an s - t -cut.
 608 Then, by adding the mass balances for all nodes in S
 609 one has $\nu = \sum_{(i,j) \in (S, \bar{S})} x_{ij} - \sum_{(i,j) \in (\bar{S}, S)} x_{ji}$ and since
 610 $x_{ij} \leq u_{ij}$ and $x_{ji} \geq 0$ the following inequality holds:
 611 $\nu \leq \sum_{(i,j) \in (S, \bar{S})} u_{ij} = u[S, \bar{S}]$. Thus the value of any flow \mathbf{x}
 612 is less or equal to the capacity of any cut in the network.
 613 If one discovers a flow \mathbf{x} whose value equals to the capaci-
 614 ty of some cut $[S, \bar{S}]$, then \mathbf{x} is a maximum flow and the
 615 cut is a minimum cut. The following implementation of the
 616 augmenting path algorithm constructs a flow whose value
 617 is equal to the capacity of a s - t -cut it defines simultane-
 618 ously. Thus it will solve the maximum flow problem (and,
 619 of course, the minimum cut problem).

620 Given a flow \mathbf{x} , the residual capacity r_{ij} of any arc
 621 $(i, j) \in A$ is the maximum additional flow that can be sent
 622 from node i to node j using the arcs (i, j) and (j, i) . The resi-
 623 dual capacity has two components: 1) $u_{ij} - x_{ij}$, the unused
 624 capacity of arc (i, j) , 2) x_{ji} the current flow on arc (j, i) ,
 625 which one can cancel to increase the flow from node i to j
 626 $r_{ij} = u_{ij} - x_{ij} + x_{ji}$. The residual network $G(\mathbf{x})$ with re-
 627 spect to the flow \mathbf{x} consists of the arcs with *positive* residual
 628 capacities. An augmenting path is a directed path from the
 629 node s to the node t in the residual network. The *capacity*
 630 *of an augmenting path* is the minimum residual capacity of
 631 any arc in this path.

Obviously, whenever there is an augmenting path in the
 residual network $G(\mathbf{x})$ the flow \mathbf{x} is not optimal. This moti-
 vates the following generic augmenting path algorithm:

algorithm Ford–Fulkerson

begin

Initially set $x_{ij} := 0, x_{ji} := 0$ for all $(i, j) \in A$;

do

construct residual network R with capacities r_{ij} ;

if there is an augmenting path from s to t in G' **then**

begin

Let r_{\min} the minimum capacity of r along this path;

Increase the flow in N along the path

by a value of r_{\min} ;

end

until no such path from s to t in G' is found;

endCE4

This algorithm is polynomial in the number of lat-
 tice sites if the distribution of capacities is discrete (bi-
 nary for instance). In the general case it has to be im-
 proved and there are indeed more efficient algorithms to
 solve this problem in polynomial time. One of them is the
 push/relabel algorithm introduced by Goldberg and Tar-
 jan [24]. It determines the maximal flow by successively
 improving a “preflow”. A preflow is an edge function $f(e)$
 that obeys the range constraint $0 \leq f(e) \leq w(e)$, but the
 conservation constraint at each node is relaxed: the sum of
 the $f(e)$ into or out of a node can be nonzero at internal
 (physical) nodes. The amount of violation of conservation
 at each node v give “excesses” $e(v)$. The basic operations of
 the algorithm, push and relabel, are used to rearrange these

CE4 Added this end. Is it correct?

662 excesses. When the preflow can no longer be improved, it
 663 can, if desired, be converted to a maximal flow, proving the
 664 correctness of the algorithm. For details see [24,25]. It can
 665 be applied in the way sketched above to compute univer-
 666 sal geometrical properties of elastic manifolds in 2 and 3
 667 dimensions [23].

668 Periodic Medium

669 The presence of a periodic background potential, like
 670 a crystal potential, has a smoothening effect on the elastic
 671 manifold and tends to lock it into one of its minima. The
 672 competition between the random potential, that roughens
 673 the manifold, and such a periodic potential might lead to
 674 a roughening transition [27,28]. In 2d this is actually not
 675 the case [29], but in 3d there is as we will see. We consider
 676 a lattice version of the Hamiltonian

$$677 \quad \mathcal{H} = \mathcal{H}_{\text{manifold}} + H_{\text{periodic}} \quad (16)$$

$$\text{with } H_{\text{periodic}} = \int d^d \mathbf{r} V_{\text{periodic}}(\phi(\mathbf{r})),$$

678 where $V_{\text{periodic}}(\phi) = -\cos \phi$ represents the periodic po-
 679 tential.

680 We introduce a discrete solid-on-solid (SOS) type in-
 681 terface model for the elastic manifold whose continuum
 682 Hamiltonian is given in Eq. (16). Locally the EM remains
 683 flat in one of periodic potential minima at $\phi = 2\pi h$ with
 684 integer h . Due to fluctuations, some regions might shift to
 685 a different minimum with another value of h to create a step
 686 (or domain wall) separating domains. To minimize the cost
 687 of the elastic and periodic potential energy in Eq. (16), the
 688 domain-wall width must be finite, say ξ_o . Therefore, if one
 689 neglects fluctuations in length scales less than ξ_o , the con-
 690 tinuous displacement field $\phi(\mathbf{r})$ can be replaced by the inte-
 691 ger height variable $\{h_{\mathbf{x}}\}$ representing a $(3+1)d$ SOS inter-
 692 face on a simple cubic lattice with sites $\mathbf{x} \in \{1, \dots, L\}^3$. The
 693 lattice constant is of order ξ_o and set to unity. The energy
 694 of the interface is given by the Hamiltonian

$$695 \quad \mathcal{H} = \sum_{\langle \mathbf{x}, \mathbf{y} \rangle} J_{(h_{\mathbf{x}}, \mathbf{x}); (h_{\mathbf{y}}, \mathbf{y})} |h_{\mathbf{x}} - h_{\mathbf{y}}| - \sum_{\mathbf{x}} V_R(h_{\mathbf{x}}, \mathbf{x}), \quad (17)$$

696 where the first sum is over nearest neighbor site pairs. Af-
 697 ter the coarse graining, the step energy $J > 0$ as well as the
 698 random pinning potential energy V_R becomes a quenched
 699 random variable distributed independently and randomly.
 700 Note a periodic elastic medium has the same Hamiltonian
 701 as in Eq. (17) with random but periodic J and V_R in
 702 h with periodicity p [30]. In this sense, the elastic mani-
 703 fold emerges as in the limit $p \rightarrow \infty$ of the periodic elastic
 704 medium.

705 To find the ground state, one maps the 3D SOS model
 706 onto a ferromagnetic random bond Ising model in $(3+1)d$
 707 hyper-cubic lattice with anti-periodic boundary conditions
 708 in the extra dimension [23] (for the 3 space direction
 709 one uses periodic boundary conditions instead). The anti-
 710 periodic boundary conditions force a domain wall into the
 711 ground state configuration of the $(3+1)d$ ferromagnet.
 712 Note that bubbles are *not* present in the ground state. A do-
 713 main wall may contain an overhang which is unphysical
 714 in the interface interpretation. Fortunately, one can forbid
 715 overhangs in the Ising model representation using a tech-
 716 nique described in [23]. If the longitudinal and transversal
 717 bond strengths are assigned with $J/2$ and $V_R/2$ occur-
 718 ring in Eq. (17), respectively, this domain wall of the
 719 ferromagnet becomes equivalent to the ground state con-
 720 figuration of (17) for the interface with the same energy.
 721 The domain wall with the lowest energy is then deter-
 722 mined exactly by using again the max-flow/min-cost algo-
 723 rithm.

724 In elastic media described by (17) the tendency of
 725 the periodic potential to lock the displacements competes
 726 with the roughening effect of the disorder. Analytically
 727 a roughening transition was predicted in [28] and the crit-
 728 ical exponents could be numerically estimated in three di-
 729 mensions [30] with the mapping and algorithm described
 730 above.

731 Random Field Ising Model

732 The random field Ising model (RFIM, for a review see [31,
 733 32]) is defined

$$734 \quad H = - \sum_{\langle ij \rangle} J_{ij} \sigma_i \sigma_j - \sum_i h_i \sigma_i \quad (18)$$

735 with $\sigma_i = \pm 1$ Ising spins, ferromagnetic bonds $J_{ij} \geq 0$ (ran-
 736 dom or uniform), $\langle ij \rangle$ nearest neighbor pairs on a d -dimen-
 737 sional lattice and at each site i a random field $h_i \in R$ that can
 738 be positive and negative. The first term prefers a ferromag-
 739 netic order, which means it tries to align all spins. The ran-
 740 dom field, however, tends to align the spins with the field
 741 which points in random directions depending on whether
 742 it is positive or negative. This is the source of competition
 743 in this model.

744 Let us suppose for the moment uniform interactions
 745 $J_{ij} = J$ and a symmetric distribution of the random fields
 746 with mean zero and variance h_r . It is established by now
 747 that in 3d (and higher dimensions) the RFIM shows fer-
 748 romagnetic long range order at low temperatures, provid-
 749 ed h_r is small enough. In 1d and 2d there is no ordered
 phase at any finite temperature. Thus in 3d one has a para-

750 magnetic/ferromagnetic phase transition along a line $h_c(T)$
 751 in the h_r - T -diagram.

752 The renormalization group picture says that the nature
 753 of the transition is the same all along the line $h_c(T)$,
 754 with the exception being the pure fixed point at $h_r = 0$ and
 755 $T_c \sim 4.51 J$. The RG flow is dominated by a zero tempera-
 756 ture fixed point at $h_c(T = 0)$. As a consequence, the critical
 757 exponents determining the critical behavior of the RFIM
 758 should be all identical along the phase transition line, in
 759 particular identical to those one obtains at zero temperature
 760 by varying h_r alone. Thus to study the universal properties
 761 of the phase transition in the RFIM one needs to calculate
 762 its ground state.

763 This optimization task is again equivalent to a maxi-
 764 mum flow problem [33,34], as in the interface model dis-
 765 cussed in the last section. Historically the RFIM was the
 766 first physical model that has been investigated with a maxi-
 767 mum flow algorithm [36]. However, here the minimum-cut
 768 is not a geometric object within the original system.

769 To map the ground state problem for the RFIM onto
 770 a max-flow-min-cut problem one proceeds in the same way
 771 as in the interface problem: One adds to extra nodes s and
 772 t and attaches spins with fixed values there (see Fig. 6):

$$773 \quad \sigma_s = +1 \quad \text{and} \quad \sigma_t = -1 \quad (19)$$

774 One connects all sites with positive random field to the
 775 node s and all sites with negative random field to t :

$$776 \quad J_{si} = \begin{cases} h_i & \text{if } h_i \geq 0 \\ 0 & \text{if } h_i < 0 \end{cases} \quad (20)$$

$$777 \quad J_{it} = \begin{cases} |h_i| & \text{if } h_i < 0 \\ 0 & \text{if } h_i \geq 0 \end{cases}$$

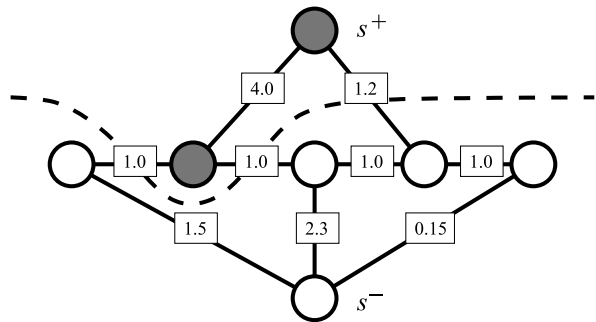
778 The a network is constructed with the set of nodes
 779 $N = \{1, \dots, L^d\} \cup \{s, t\}$ and the set of (forward and back-
 780 ward) arcs $A = \{(i, j) | i, j \in N, J_{ij} > 0\}$. Each of them has
 781 a capacity $u_{ij} = J_{ij}$. The energy or cost function can be
 written as

$$782 \quad E = - \sum_{(i,j) \in A} J_{ij} \sigma_i \sigma_j \quad (21)$$

783 or, by denoting the set $S = \{i \in N | \sigma_i = +1\}$ and $\bar{S} = N \setminus S$

$$784 \quad E(S) = -C + 2 \sum_{(i,j) \in (S, \bar{S})} J_{ij} \quad (22)$$

785 with $C = \sum_{(i,j) \in A} J_{ij}$. The problem is reduced to the prob-
 786 lem of finding a minimum s - t -cut as in (14). The difference
 787 to the interface problem is that now the extra bonds con-
 788 necting the two special nodes s and t with the original lat-
 789 tice do not have infinite capacity: they can lie in the cut,



Optimization Problems and Algorithms from Computer Science, Figure 6

Representation of the ground state problem for the RFIM as an RBIM domain wall or minimum-cut problem. The physical spins are the five nodes in the single row in the figure, while the fixed external spins are s^+ and s^- . The physical RFIM coupling $J = 1.0$. A spin with $h_i > 0$ ($h_i < 0$) is connected by an auxiliary coupling of strength h_i ($-h_i$) to s^+ (s^-). The weights of each bond are indicated: the random fields are, from left to right, $h = -1.5, +4.0, -2.3, +1.2$, and 0.15 . In the ground state, the interfacial energy between up-spin and down-spin domains is minimized, i. e., the spins are partitioned into two sets with minimal total cost for the bonds connecting the two sets. The dashed curve indicates the minimal weight cut. The white (dark) nodes indicate up (down) spins in the ground state configuration

790 namely whenever it is more favorable not to break a fer-
 791 romagnetic bond but to disalign a spin with its local ran-
 792 dom field. In the extended graph the s - t -cut again forms
 793 connected interface, however, in the original lattice (with-
 794 out the bonds leading to and from the extra nodes) the
 795 resulting structure is generally *disconnected*, a multicom-
 796 ponent interface. Each single component surrounds a con-
 797 nected region in the original lattice containing spins, which
 798 all point in the same direction. In other words, they form
 799 ferromagnetically ordered domains separated by domain
 800 walls given by the subset of the s - t -cut that lies in the orig-
 801 inal lattice.

802 In passing we note that diluted Ising antiferromagnets
 803 in a homogeneous external field (DAFF) map straightfor-
 804 wardly onto a RFIM if the underlying lattice is bipartite.
 805 The 3d DAFF on a simple cubic lattice is defined by

$$806 \quad H = + \sum_{(ij)} J_{ij} \varepsilon_i \varepsilon_j \sigma_i \sigma_j - \sum_i h_i \varepsilon_i \sigma_i \quad (23)$$

807 where $\sigma_i = \pm 1$, $J_{ij} \geq 0$, (ij) are nearest neighbor pairs on
 808 a simple cubic lattice, and $\varepsilon_i \in \{0, 1\}$ with $\varepsilon_i = 1$ with prob-
 809 ability c , representing the concentration of spins. Because
 810 of the plus sign in front of the first term in (23) all interac-
 811 tions are antiferromagnetic, the model represents a diluted
 812 antiferromagnet, for which many experimental realizations
 813 exist (e.g. $\text{Fe}_c \text{Zn}_{1-c} \text{F}_2$). Now that neighboring spins tend

814 to point in opposite directions due to their antiferromag- 853
 815 netic interaction a uniform field competes with this ordering 854
 816 tendency by trying to align them all. On a bipartite lat- 855
 817 tice in zero external field the ground state would be antifer- 856
 818 romagnetic, which means that one can define two bipartite 857
 819 sublattices A and B . One defines new spin and field vari- 858
 820 ables via

$$\begin{aligned} \sigma'_i &= \begin{cases} +\sigma_i & \text{for } i \in A \\ -\sigma_i & \text{for } i \in B \end{cases} \\ h'_i &= \begin{cases} +\varepsilon_i h_i & \text{for } i \in A \\ -\varepsilon_i h_i & \text{for } i \in B \end{cases} \end{aligned}$$

822 Since $\sigma'_i \sigma'_j = -\sigma_i \sigma_j$ for all nearest neighbor pairs (ij) one 859
 823 can write (23) as

$$H = - \sum_{(ij)} J'_{ij} \sigma'_i \sigma'_j - \sum_i h'_i \sigma'_i \quad (24)$$

825 with $J'_{ij} = J_{ij} \varepsilon_i \varepsilon_j$. This is again a RFIM and ground states 860
 826 can be computed with the max-flow technique.

827 The main focus of the application of the max-flow-min- 861
 828 cut algorithm to the RFIM is the phase transition in the 862
 829 three-dimensional model occurring at a critical disorder 863
 830 strength h_c at zero temperature, which separates a param- 864
 831 agnetic phase for large disorder strength from a ferromag- 865
 832 netic phase. The maximum flow algorithm has first been 866
 833 used by Ogielski [36] to calculate the critical exponents of 867
 834 the RFIM via the finite size scaling. More accurate estimates 868
 835 were obtained more recently by Middleton and Fisher [35], 869
 836 where also an detailed discussion of the problems and con- 870
 837 flicting results about the RFIM universality class is pro- 871
 838 vided. For Gaussian random fields (with variance h^2) they 872
 839 find for the finite size scaling of magnetization $m = [S_i]_{av}$ 873
 840 and specific heat $c = N^{-1} dE/dT$ and

$$\begin{aligned} m &\sim L^{-\beta/\nu}, \\ c &\sim L^{\alpha/\nu}, \end{aligned} \quad (25)$$

842 with the magnetization exponent $x = \beta/\nu = 0.012 \pm 0.004$ 874
 843 the correlation length exponent $\nu = 1.37 \pm 0.09$, and the 875
 844 specific heat exponent $\alpha = -0.07 \pm 0.17$. Note that the mag- 876
 845 netization exponent is very close to zero, which means that 877
 846 the transition is hard to discriminate from a first order tran- 878
 847 sition. Also the specific heat exponents is close to zero and 879
 848 slightly negative, implying a lack of divergence of the spe- 880
 849 cific heat at the transition.

850 The Spin Glass Problem

851 Spin glasses are the prototypes of (disordered) frustrated 881
 852 systems (see [37]). In the models discussed up to now,

the frustration was caused by two separate terms of dif- 853
 854 ferent physical origin (interactions and external fields or 854
 855 boundary conditions). Spin glasses are magnetic systems 855
 856 in which the magnetic moments interact ferro- or antifer- 856
 857 romagnetically in a random way, as in the following Ed- 857
 858 wards-Anderson Hamiltonian for a short ranged Ising spin 858
 859 glass (SG)

$$H = - \sum_{(ij)} J_{ij} \sigma_i \sigma_j, \quad (26)$$

where $\sigma_i = \pm 1$, (ij) are nearest neighbor interactions on a d - 861
 862 dimensional lattice and the interaction strengths $J_{ij} \in R$ are 862
 863 unrestricted in sign. In analogy to Eq. (14) one shows that 863
 864 the problem of finding the ground state is again equivalent 864
 865 to finding a minimal cut $[S, \bar{S}]$ in a network

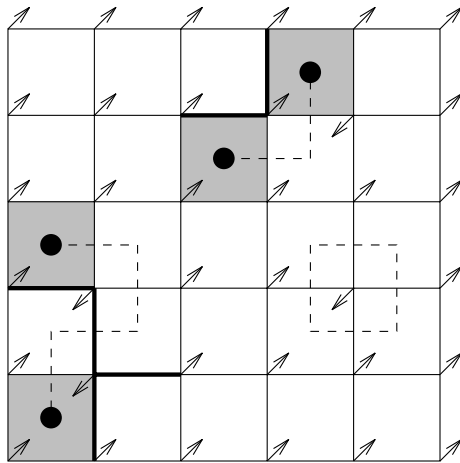
$$\min_{\underline{\sigma}} \{H'(\underline{\sigma})\} = \min_{[S, \bar{S}]} \sum_{(i,j) \in (S, \bar{S})} J_{ij}, \quad (27)$$

again $H' = (H + C)/2$ with $C = \sum_{(ij)} J_{ij}$. However, now 867
 868 the capacities $u_{ij} = J_{ij}$ of the underlying network are *not* 868
 869 non-negative any more, therefore it is *not* a minimum-cut 869
 870 problem and thus it is also not equivalent to a maximum 870
 871 flow problem, which we know how to handle efficiently.

872 It turns out that the spin glass problem is *much* harder 872
 873 than the questions we have discussed so far. In general (i. e. 873
 874 in any dimension larger than two and also for 2d in the 874
 875 presence of an external field) the problem of finding the SG 875
 876 ground state is \mathcal{NP} -complete [42], which means in essence 876
 877 that no polynomial algorithm for it is known (and also that 877
 878 chances to find one in the future are marginal). Neverthe- 878
 879 less, some extremely efficient algorithms for it have been 879
 880 developed [38,39], which have a non-polynomial bound 880
 881 for their worst case running-time but which terminate (i. e. 881
 882 find the optimal solution) after a reasonable computing 882
 883 time for pretty respectable system sizes.

884 Two Dimensions, Planar Graph

885 First we discuss the only non-trivial case that can be 885
 886 solved with a polynomial algorithm: the two-dimensional 886
 887 Ising SG on a planar graph. This problem can be shown to 887
 888 be equivalent to finding a minimum weight perfect match- 888
 889 ing, which can be solved in polynomial time. We do not 889
 890 treat matching problems and the algorithms to solve them 890
 891 in this lecture (see [4,40,41]), however, we would like to 891
 892 present the idea [42]. To be concrete let us consider a square 892
 893 lattice with free boundary conditions. Given a spin config- 893
 894 uration $\underline{\sigma}$ (which is equivalent to $-\underline{\sigma}$) we say that an edge 894
 895 (or arc) (i,j) is satisfied if $J_{ij} \sigma_i \sigma_j > 0$ and it is *unsatisfied* 895
 896 if $J_{ij} \sigma_i \sigma_j < 0$. Furthermore we say a plaquette (i. e. a unit 896
 897 cell of the square lattice) is *frustrated* if it is surrounded by



Optimization Problems and Algorithms from Computer Science, Figure 7
 Two-dimensional Ising spin glass with $\pm J$ couplings: *Thin lines, are positive interactions, thick lines are negative interactions, ↗ means $\sigma_i = +1$, ↖ means $\sigma_i = -1$, shaded faces are frustrated plaquettes, broken lines cross unsatisfied edges*

an odd number of negative bonds (i. e. $J_{ij} \cdot J_{jk} \cdot J_{kl} \cdot J_{li} < 0$ with i, j, k and l the four corners of the plaquette)). There is a one-to-one correspondence between equivalent spin configurations ($\underline{\sigma}$ and $-\underline{\sigma}$) and sets of unsatisfied edges with the property that on each frustrated (unfrustrated) plaquette there is an odd (even) number of unsatisfied edges. See Fig. 7 for illustration.

Note that

$$H(\underline{\sigma}) = -C + 2 \sum_{\text{unsatisfied edges}} |J_{ij}|. \quad (28)$$

which means that one has to minimize the sum over the weights of unsatisfied edges. A set of unsatisfied edges will be constituted by a set of paths (in the dual lattice) from one frustrated plaquette to another and a set of closed circles (see Fig. 7). Obviously the latter always increase the energy so that we can neglect them. The problem of finding the ground state is therefore equivalent to finding the minimum possible sum of the weights of these paths between the frustrated plaquettes. This means that we have to *match* the black dots in the Fig. 7 with one another in an optimal way. One can map this problem on a minimum weight **perfect matching** problem (a perfect matching of a graph $G = (N, A)$ is a set $M \subseteq A$ such that each node has only one edge of M adjacent to it). This can be solved in polynomial time (see [42] for further details).

Note that for binary couplings, i. e. $J_{ij} = \pm J$, where $J_{ij} = +J$ with probability p the weight of a matching is simply proportional to the sum of the lengths of the various

paths connecting the centers of the frustrated plaquettes, which simplifies the actual implementation of the algorithm. In [43] the 2d $\pm J$ spin glass and the site disordered SG has been studied extensively with this algorithm. The site disordered spin glass is defined as follows: occupy the sites of a square lattice randomly with A (with concentration c) and B (with concentration $1 - c$) atoms. Now define the interactions J_{ij} between neighboring atoms: $J_{ij} = -J$ if on both sites are A-atoms and J_{ij} otherwise.

The main application of this algorithm is directed towards studying domain walls in spin glasses since they provide informations on the low temperature behavior and the stability of the ground state with respect to thermal fluctuations. Domain walls can be induced by applying two different boundary conditions to the system (usually periodic and anti-periodic), their energy is simply the difference between the energies of the ground states with the two different boundary conditions. The domain wall energy of the two-dimensional spin glass model with Gaussian couplings scales like

$$\Delta E \sim L^\theta, \quad (29)$$

where the stiffness exponent is $\theta = -0.282$ (see [44] for a survey). The negativity of this exponent indicates the absence of stable spin glass phase at any non-vanishing temperature in the 2d spin glass model. Recently also the fractal properties of the domain walls in 2d spin glasses with Gaussian couplings became important: They have a fractal dimension of $d_f = 1.27(1)$ and it was argued [45] that they might be a realization of a stochastic Loewner evolution (see [46] for a review) realized in disordered systems.

Three Dimensions, Non-planar Graphs

As we mentioned, in any other case except the planar lattice situation discussed above the spin glass problem is \mathcal{NP} -hard. In what follows we would like to sketch the idea of an efficient but non-polynomial algorithm [39]. To avoid confusion with the minimum cut problem we discussed in connection with maximum flows one calls the problem (27) a max-cut problem (since finding the minimum of H is equivalent to finding the maximum of $-H$).

Let us consider the vector space R^A . For each cut $[S, \bar{S}]$ define $\chi^{(S, \bar{S})} \in R^A$, the incidence vector of the cut, by $\chi_e^{(S, \bar{S})} = 1$ for each edge $e = (i, j) \in (S, \bar{S})$ and $\chi_e^{(S, \bar{S})} = 0$ otherwise. Thus there is a one-to-one correspondence between cuts in G and their $\{0, 1\}$ -incidence vectors in R^A . The *cut-polytope* $P_C(G)$ of G is the convex hull of all incidence vectors of cuts in G : $P_C(G) = \text{conv} \{ \chi^{(S, \bar{S})} \in R^A \mid S \subseteq A \}$. Then the max-cut problem can be written as a *linear pro-*

972 *gram*

$$973 \quad \max \{ \underline{u}^T \underline{x} \mid \underline{x} \in P_C(G) \} \quad (30)$$

974 since the vertices of $P_C(G)$ are cuts of G and vice versa. Lin-
 975 ear programs usually consist of a linear cost function $\underline{u}^T \underline{x}$
 976 that has to be maximized under the constraint of various
 977 inequalities defining a polytope in R^n (i. e. the convex hull
 978 of finite subsets of R^n) and can be solved for example by the
 979 simplex method, which proceeds from corner to corner of
 980 that polytope to find the maximum (see e. g. [40,41,48]).
 981 The crucial problem in the present case is that it is \mathcal{NP} -
 982 hard to write down all inequalities that represent the cut
 983 polytope $P_C(G)$.

984 It turns out that also *partial* systems are useful, and this
 985 is the essential idea for an efficient algorithm to solve the
 986 general spin glass problem as well as the traveling sales-
 987 man problem or other so called mixed integer problems
 988 (i. e. linear programs where some of the variables x are
 989 only allowed to take on some integer values, like 0 and 1 in
 990 our case) [7,47]. One chooses a system of linear inequali-
 991 ties L whose solution set $P(L)$ contains $P_C(G)$ and for which
 992 $P_C(G) = \text{convex hull} \{ \mathbf{x} \in P(L) \mid x \text{ integer} \}$. In the present
 993 case these are $0 \leq x \leq 1$, which is trivial, and the so called
 994 cycle inequalities, which are based on the observation that
 995 all cycles in G have to intersect a cut an even number of
 996 times. The most remarkable feature of this set L of inequali-
 997 ties is the following:

998 The separation problem for a set of inequalities L con-
 999 sists in either proving that a vector x satisfies all inequali-
 1000 ties of this class or to find an inequality that is violated
 1001 by \mathbf{x} . A linear program can be solved in polynomial time
 1002 if and only if the separation problem is solvable in poly-
 1003 nomial time [49]. The separation problem for the cycle in-
 1004 equalities can be solved in polynomial time by the *cutting*
 1005 *plane algorithm* which, starting from some small initial set
 1006 of inequalities, generates iteratively new inequalities until
 1007 the optimal solution for the actual subset of inequalities is
 1008 feasible. Note that one does not solve this linear program
 1009 by the simplex method since the cycle inequalities are still
 1010 too numerous for this to work efficiently.

1011 Due to the insufficient knowledge of the inequalities
 1012 that are necessary to describe $P_C(G)$ completely, one may
 1013 end up with a non-integral solution \mathbf{x}^* . In this case one
 1014 *branches* on some fractional variable x_e (i. e. a variable with
 1015 $x_e^* \notin \{0, 1\}$), creating two subproblems in one of which x_e
 1016 is set to 0 and in the other x_e is set to 1. Then one applies the
 1017 cutting plane algorithm recursively for both subproblems,
 1018 which is the origin of the name *branch-and-cut*. Note that
 1019 in principle this algorithm is not restricted to any dimen-
 1020 sion, boundary conditions, or to the fieldless case. How-
 1021 ever, there are realizations of it that run fast (e. g. in 2d) and

others that run slow (e. g. in 3d) and it is ongoing research
 to improve on the latter, for an overview over the current
 status see [47].

Potts Free Energy and Submodular Functions

The problem addressed in this chapter is not a low tem-
 perature problem but concerns the computation of the free
 energy of a Potts model (see [50] for a review) at *any tem-*
perature, including some phase transition temperatures. To
 transform the problem of computing the free energy into an
 optimization problem (i. e. find a minimum in a finite set),
 one needs to take some limit. Usually this is a zero temper-
 ature limit as it was for all applications discussed so far in
 this article. Here this will be the limit of an *infinite number*
of states.

Consider the q -state Potts model on a d -dimensional
 hyper-cubic lattice with periodic boundary conditions def-
 ined by the Hamiltonian:

$$H = - \sum_{\langle ij \rangle} J_{ij} \delta(\sigma_i, \sigma_j), \quad (31)$$

where σ_i are q -state Potts variables ($\sigma_i \in \{1, \dots, q\}$) located
 at lattice sites i , the sum goes over all nearest neighbor pairs
 $\langle ij \rangle$ of the lattice, and $J_{ij} > 0$ are ferromagnetic couplings
 (not that $\delta(\sigma, \sigma')$ is the Kronecker-delta, which means
 $\delta(\sigma, \sigma') = 1$ for $\sigma = \sigma'$ and $\delta(\sigma, \sigma') = 0$ for $\sigma \neq \sigma'$). The case
 $q = 2$ corresponds to the Ising model. In the random bond
 Potts model, which is of interest here, the couplings J_{ij}
 are random variables. In $d \leq 2$ dimensions the Potts model
 has phase transition at some critical temperature T from
 a paramagnetic to a ferromagnetic phase. Thermodynamic
 properties of the q -state Potts model are computed via its
 partition function

$$\mathcal{Z} = \sum_{\{\sigma\}} \exp \left(\sum_{ij} -\beta J_{ij} \delta(\sigma_i, \sigma_j) \right). \quad (32)$$

The first sum runs over all possible spin configuration, i. e.
 it involves q^N terms, where N is the number of spins in the
 system and $\beta = 1/T$ is the inverse temperature.

In the so-called random cluster representation [51] the
 partition sum can be written as a sum over all subsets $U \subseteq E$
 of the set of edges (or bonds)

$$\begin{aligned} \mathcal{Z} &= \sum_{\{\sigma\}} \prod_{ij} \exp(-\beta J_{ij} \delta(\sigma_i, \sigma_j)) \\ &= \sum_{\{\sigma\}} \prod_{ij} (1 + v_{ij} \delta(\sigma_i, \sigma_j)) \end{aligned}$$

where $v_{ij} = \exp(\beta J_{ij}) - 1$. Note that the Kronecker-delta
 can only take on the values zero and one by which it is

possible to identify $\exp(J\delta) = 1 + \delta(\exp(J) - 1) = 1 + \nu\delta$. Again one can regard the lattice as a graph $G = (V, E)$, where the sites and the bonds of the lattice are the vertices V and the edges E of the graph. Then a careful book-keeping of the terms in the development of the above expression leads to:

$$Z = \sum_{G' \subseteq G} q^{c(G')} \prod_{e \in G'} v_e, \quad (33)$$

where G' denotes any subgraph of G , i. e. a graph, possibly not connected (but all vertices are kept), where some edges of G have been deleted (there are 2^m subgraphs where m is the number of edges of G). $c(G')$ is the number of connected components of the subgraph G' . For example for the empty subgraph $G' = \emptyset$ the number of connected components is the number of sites, while for $G' = G$ it is one. The product in (33) is over all the edges in G' with the convention that the product over an empty set is one. If the parameter β is small (i. e. high temperature) then the parameters v_{ij} are small and, summing in (33), only the subgraphs with few edges provides an approximation to the partition function: this is a high temperature development. Note also the way the parameter q appears in (33): it can be extended to non integer values, relating the Potts model to other problems (percolation, etc ...) [58].

Following [52] one can map the computation of the partition function Z of any ferromagnetic Potts model in the limit $q \rightarrow \infty$ onto an optimization problem by introducing another parametrization of the couplings with new variables w_e defined by

$$v_e = q^{w_e}.$$

Inserting this expression in (33) one gets $Z = \sum_{G' \subseteq G} q^{c(G') + \sum_{e \in G'} w_e}$, and defining $f(G) = c(G) + \sum_{e \in G} w_e$:

$$Z = \sum_{G' \subseteq G} q^{f(G')}.$$

In the limit $q \rightarrow \infty$ only the subgraphs G^* maximizing $f(G)$ will contribute, and computing the partition function of the Potts model in the infinite number of states limit amounts to finding the subgraphs G' of the graph G maximizing the function f , i. e. minimizing the function [52]:

$$f_P(G') = - \left(c(G') + \sum_{e \in G'} w_e \right). \quad (34)$$

It turns out that this function has a property which allows to minimize it very efficiently: it is a *submodular function*.

Submodular Functions

The concept of a submodular function in discrete optimization appears to be in several respects analogous to that of a convex function in continuous optimization. In many combinatorial theorems and problems, submodularity is involved, in one form or another, and submodularity often plays an essential role in a proof or an algorithm. Moreover, analogous to the fast methods for convex function minimization, it turns out that submodular functions can also be minimized fast, i. e. in polynomial time.

Submodularity is a special property of *set functions*, which are defined as follows: Let V be a finite set and $2^V = \{X \mid X \subseteq V\}$ be the set of all the subsets of V . A function $f: 2^V \rightarrow \mathbb{R}$ is called a set function.

Now a set function f is **submodular** if for all subsets $A \subseteq V$ and $B \subseteq V$:

$$f(A) + f(B) \geq f(A \cap B) + f(A \cup B). \quad (35)$$

It is simple to show that a function f is submodular if and only if for any subsets $S \subseteq R \subseteq V$ and for any $x \in V$:

$$f(S \cup \{x\}) - f(S) \geq f(R \cup \{x\}) - f(R). \quad (36)$$

This means intuitively that adding an element to a "small" ensemble S (since $S \subseteq R$) has more effect than adding to a "large" ensemble R .

The function (34) $f_P(A) = -(c(A) + w(A))$ is submodular, because the function $-c(A)$ is submodular (and the function $w(A)$ is modular: Take two sets of edges $A \subseteq B$ and an edge e . Inspecting the three possible cases: $e \in A$, $e \notin A$ and $e \in B$, $e \notin A$ and $e \notin B$ one sees that $c(A \cup \{e\}) - c(A) \leq c(B \cup \{e\}) - c(B)$, which is the reverse of (36), so that the function $-c$ is a submodular function. Note that $c(E')$ with $E' \subseteq E$ counts the number of connected components of the graph G' that contains *all* vertices V of the complete graph but only the edges in E' . Thus adding an edge will never increase the number of components.

On the other hand it is straightforward to see that the function $w(G) = \sum_{e \in G} w_e$ verifies $w(A \cup C) + w(A \cap C) = w(A) + w(C)$. It is a so-called *modular* function. Consequently the function (34) f_P is a submodular function. In summary we are looking for the sets of edges minimizing the submodular function f_P for which a *strongly polynomial* algorithm has been recently discovered.

In passing we note that we encountered other examples of submodular functions already in the preceding sections, namely the function that defines the costs of cuts in a graph with positive edge weights, which occurs the interface problem and the random field Ising model in the last sections: Take a graph $G = (V, E)$ and define C to be a function of the subsets of the V and $C(U \subseteq V)$ is the

1151 number of edges having exactly one end in U . This func-
 1152 tion can be generalized to the case where the edges are di-
 1153 rected and weighted, i. e. each edge carries an arrow and
 1154 a positive number. The function $C(U \subseteq V)$ is then the sum
 1155 of the weight of the edges having the beginning vertex in U
 1156 and the ending vertex not in U . This kind of function is
 1157 generally called a “cut” and is submodular.

1158 **Minimization of Submodular Function**

1159 The minimization of any submodular function can be
 1160 done in polynomial time. This was first published in refer-
 1161 ence [54] in 1981. In this paper the authors utilize the so-
 1162 called ellipsoid method. However this method is not a com-
 1163 binatorial one and is far from being efficient. In that respect
 1164 this result was not quite satisfactory at least for the prac-
 1165 tical applications. Eighteen years later, Iwata–Fleischer–
 1166 Fujishige [55], and independently Schrijver [56] discovered
 1167 a combinatorial method which is fully satisfactory from the
 1168 theoretical, as well as from the practical, point of view.

1169 The general method uses a mathematical program-
 1170 ming formulation. The problem is algebraically expressed
 1171 as a linear program, i. e. a set of variables y_S associated to
 1172 each subset $S \subset V$ is introduced, these variables are sub-
 1173 jected to constraints and a linear function F of these vari-
 1174 ables is to be minimized. The constraints include a set of
 1175 linear equations and the condition that each of the y_S is
 1176 zero or one. This last condition is in general extremely dif-
 1177 ficult to realize. However, it turns out that a theorem due
 1178 to Edmonds [57] indicates this condition can be simply
 1179 dropped, and that automatically the set of values y_S which
 1180 minimize F will all be zero or one! Actually only one vari-
 1181 able $y_{S^*} = 1$ will be non zero and it is precisely associated to
 1182 the optimal set. Combined with the dual version of this lin-
 1183 ear program, it provides a characterization of the optimal
 1184 set.

1185 The general algorithm mentioned above can be applied
 1186 to minimize (34), however, due to the specific form of the
 1187 function to minimize, a more suitable method does exist.
 1188 For this a property that is true for any submodular function
 1189 is useful. To emphasize that the function f to minimize is
 1190 defined on all the subsets of a set E we will label f with the
 1191 index E as f_E . Let us now consider a subset $F \subseteq E$; one can
 1192 define a set function on F by $f_F(A) = f_E(A)$ for any $A \subseteq F$.
 1193 If the function f_E is submodular then its restriction f_F is
 1194 also submodular. We have the following property:

1195 Let $F \subseteq E$ and $e \in E$, if A_F is an optimal set of the set
 1196 function f_F defined on F , then there will be an optimal set
 1197 $A_{F \cup \{e\}}$ of the function $f_{F \cup \{e\}}$ defined on $F \cup \{e\}$ such that
 1198 $A_F \subseteq A_{F \cup \{e\}}$.

To make the notation simpler we denote the function
 $f_{F \cup \{e\}}$ on $F \cup \{e\}$ by f_1 . Let A be an optimal set of f_F on F
 and B an optimal set of f_1 on $F \cup \{e\}$. One has

$$f_1(A \cup B) \leq f_1(A) + f_1(B) - f_1(A \cap B) \quad (37)$$

since f_1 is submodular. But $f_1(A) = f_F(A)$ and $f_1(A \cap B) =$
 $f_F(A \cap B)$ since both A and $A \cap B$ are in A . Since A is
 an optimal set one has $f_F(A) \leq f_F(A \cap B)$ and conse-
 quently $f_1(A) - f_1(A \cap B) \leq 0$. Inserting this last inequal-
 ity into (37) one finds that $f_1(A \cup B) \leq f_1(B)$ which proves
 that $A \cup B$ is one of the optimal sets (Q.E.D.).

This property has an important consequence. Indeed let
 us suppose that the optimal set has been found for a sub-
 set F of E . Then all the elements of E which have been se-
 lected as belonging to the optimal set of F will still belong
 to one optimal set of all the sets $G \supseteq F$. In other words, let
 us find the optimal set for $\{e_0, e_1\}$ where e_0 and e_1 are arbi-
 trary elements of E ; then if we find that any of these two ele-
 ments belongs to the optimal set, it will belong to one opti-
 mal set for $F \subseteq E$! Such an algorithm which makes a definit-
 ive choice at each step is called a *greedy* algorithm.

Based on this observation an efficient algorithm for the
 minimization of (34) was developed in [59], see also [60].

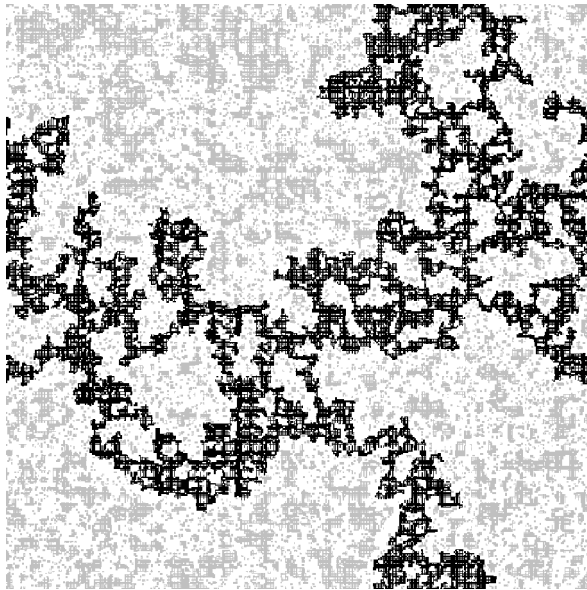
Results

The algorithm based on the ideas mentioned before and
 presented in detail in [59,60], was applied to various two
 dimensional and three dimensional lattices. A realization
 of the disorder is chosen accordingly to a probability dis-
 tribution. In practice all the weights $w(e)$ on the edge e are
 rational numbers with a common integer denominator q .
 In other words, we choose an integer $p(e)$ for each edge and
 set $w(e) = p(e)/q$. To work only with integers one maxi-
 mizes the product qf :

$$qf(A) = qC(A) + \sum_{e \in A} p(e).$$

It is clear that if q is small compare to all the $p(e)$, then all
 the weights $w(e)$ will be large and the optimal set will be the
 set of all edges. On the contrary if q is large all the weights
 will be small and the optimal set will be empty. These two
 situations are easy to handle. Between this two limits the
 optimal set grows, and for a precise value q_c of q , which
 depends on the lattice, the optimal set percolates. This value
 corresponds to a phase transition. Depending on the lattice
 under consideration and on the distribution of the random
 variables $p(e)$ this transition can be first or second order.

In Fig. 8, one optimal set is shown for a lattice where
 each edge carries a weight $1/6$ or $5/6$ with probability one
 half (i. e. it is a critical point). The edges from the optimal



Optimization Problems and Algorithms from Computer Science, Figure 8

A 512×512 lattice. The edges of the optimal set belonging to the percolating cluster are shown in *black*, and the edges of the optimal set not belonging to the optimal set are in *gray* (from [60])

1245 set belonging to the percolation cluster are shown in black,
 1246 while the others are shown in gray. The percolation cluster,
 1247 which is the largest connected component in the optimal
 1248 subgraph $G' \subseteq G$ is fractal with a fractal dimension
 1249 $d_f = 1.809$ that is related to the critical exponent $x = \beta/\nu$
 1250 for the magnetization of the random bond $q \rightarrow \infty$ Potts
 1251 model (31) in two dimensions via $x = 2 - d_f = 0.191$. Sur-
 1252 prisingly this agrees within the error bars with the magneti-
 1253 zation exponent $x = (3 - \sqrt{5})/4$ of the random transverse
 1254 Ising chain [62], which is a one-dimensional quantum spin
 1255 model. A discussion of this observation and details of the
 1256 computations can be found in [61].

1257 Future Directions

1258 We have reviewed several applications of polynomial opti-
 1259 mization algorithms from computer science to disordered
 1260 systems in statistical physics. They were used extensively in
 1261 the recent years to compute numerically universal proper-
 1262 ties like critical exponents, domain wall exponents and ge-
 1263 ometrical features like roughness and stiffness with much
 1264 higher precision than with Monte-Carlo methods, which
 1265 suffer notoriously from equilibration problems. A number
 1266 of important issues, which were controversially debated
 1267 within different analytical could be clarified, numerically,
 1268 in this way – as for instance the nature of the low tempera-

ture phase of the superrough phase in the two-dimensional
 Bragg glass [19,63], the absence of a stable glass phase in the
 strongly screened vortex glass model [21] and the issue of
 many states in various two-dimensional glassy models [64].
 Other questions still remain to be answered, as for exam-
 ple the phenomenon of an apparent non-universality in the
 three-dimensional random field Ising model [65].

NP-hard problems occurring in the statistical physics
 of disordered systems, still remain a challenge: Examples
 are the computation of ground states of spin glass mod-
 els on non-planar graphs, like the three-dimensional spin
 glass or the random field Potts model for three or more
 Potts states [66]. Stochastic optimization techniques like
 hysteretic optimization [67] or extremal optimization [68]
 have reached a high level of sophistication but naturally
 suffer from the lack of a proof of optimality of the result-
 ing solution. Progress in the development of exact and ef-
 ficient algorithm that can handle sufficiently large system
 sizes to perform a reliable finite size scaling analysis is be-
 ing made [47] and highly rewarding.

The cross-fertilization between computer science and
 statistical physics is also fruitful in the other direction:
 Phase transitions that occur in some combinatorial opti-
 mization problems like the satisfiability problem (SAT)
 were studied intensively in recent years by physicists and
 remarkable progress has been achieved in understanding
 it and inventing efficient algorithms. These developments
 were not covered in this article, excellent introductions can
 be found in [69].

Bibliography

Primary Literature

1. Rieger H (1998) In: Kertesz J, Kondor I (eds) Lect Note Phys 501:122–158
2. Alava M, Duxbury P, Moukarzel C, Rieger H (2000) In: Domb C and Lebowitz JL (eds) Phase Transit Crit Phenom 18:141–317
3. Hartmann A, Rieger H (2002) Optimization in Physics. Wiley VCH, Darmstadt **TSS**
4. Papadimitriou CH Steiglitz K (1998) Combinatorial Optimization. Dover Publications, Mineola (NY)
5. Cook WJ, Cunningham WH, Pulleyblank WR, Schrijver A (1998) Combinatorial Optimization. Wiley, New York
6. Korte B, Vygen J (2000) Combinatorial Optimization. Springer, Berlin, Heidelberg
7. Lawler EL, Lenstra JK, Rinnooy Kan AHG, Shmoys DB (1990) The Travelling Salesman Problem. Wiley, Chichester
8. Press WH, Teukolsky SA, Vetterling WT, Flannery BP (1995) Numerical Recipes in C. Cambridge University Press, Cambridge
9. Kirkpatrick S, Gelatt CD Jr, Vecchi MP (1983) Science 220:671
10. Halpin-Healy T, Zhang Y-C (1995) Phys Rep 254:215 **TSS**
11. Peng C-K, Havlin S, Schwartz M, Stanley HE (1991) Phys Rev A 44:2239; Pang N-N, Yu Y-K, Halpin-Healy T (1995) Phys Rev E 52:3224 **TSS**

TSS Please provide title of the article.

12. Marsili M, Zhang Y-C (1998) Phys Rev E 57:4814; Schwartz N, Nazaryev AL, Havlin S (1998) Phys Rev E 58:7642 **TSS** 1322
13. Schorr R, Rieger H (2003) Europ Phys J 33:347 **TSS** 1323
14. For a review see Blatter G et al (1994) Rev Mod Phys 66:1125 **TSS** 1324
15. Doi M, Edwards SF (1986) The Theory of Polymer Dynamics. Oxford University Press, Oxford 1326
16. Drossel B, Kardar M (1996) Phys Rev E 53:5861 **TSS** 1328
17. Bikbov R, Nechaev S (2001) Phys Rev Lett 87:150602 **TSS** 1329
18. Petäjä V, Alava M, Rieger H (2004) Europhys Lett 66:778 **TSS** 1330
19. Rieger H, Blasum U (1997) Phys Rev B 55:7394R; Pfeiffer F, Rieger H (2000) J Phys A 33:2489 **TSS** 1331
20. Bokil HS, Young AP (1995) Phys Rev Lett 74:3021 **TSS** 1333
21. Kisker J, Rieger H (1998) Phys Rev B 58:R8873; Pfeiffer F, Rieger H (1999) Phys Rev B 60:6304 **TSS** 1334
22. Pfeiffer FO, Rieger H (2002) J Phys C 14:2361; Pfeiffer FO, Rieger H (2003) Phys Rev E 67:056113 **TSS** 1337
23. Middleton AA (1995) Phys Rev E 52:R3337; McNamara D, Middleton AA, Zeng C (1999) Phys Rev B 60:10062 **TSS** 1339
24. Goldberg AV, Tarjan RE (1988) J Assoc Comput Mach 35:921 **TSS** 1341
25. Ahuja RK, Magnati TL, Orlin JB (1993) Network Flows. Prentice Hall, London 1343
26. Nattermann T (1990) Phys Rev Lett 64:2454; Giarmachi T, Le Doussal P (1994) Phys Rev Lett 72:1530; (1995) Phys Rev B 52:1242 **TSS** 1344
27. Bouchaud J-P, Georges A (1992) Phys Rev Lett 68:3908 **TSS** 1347
28. Emig T, Nattermann T (1997) Phys Rev Lett 79:5090; (1999) Eur J Phys B 8:525 **TSS** 1349
29. Seppälä ET, Alava MJ, Duxbury PM (2001) Phys Rev E 63:036126 **TSS** 1350
30. Noh JD, Rieger H (2001) Phys Rev Lett 87:176102; (2002) Phys Rev E 66:036117 **TSS** 1352
31. Rieger H (1995) Monte Carlo simulations of Ising spin glasses and random field systems. In: Annual Reviews of Computational Physics II. World Scientific, Singapore, pp 295–341 1354
32. Nattermann T (1998) In: Young AP (ed) Spin Glasses and Random Fields. World Scientific, Singapore 1357
33. Anglés d'Auriac JC, Preissman M, Rammal R (1985) J Phys (France) Lett 46:L173 **TSS** 1359
34. Barahona F (1985) J Phys A 18:L673 **TSS** 1360
35. Middleton AA, Fisher DS (2002) Phys Rev 65:13411 **TSS** 1362
36. Ogielski AT (1986) Phys Rev Lett 57:1251 **TSS** 1363
37. Kawashima N, Rieger H (2004) In: Diep HT (ed) Frustrated Spin Systems. World Scientific, Singapore 1364
38. Grötschel M, Jünger M, Reinelt G (1985) In: van Hemmen L, Morgenstern I (eds) Heidelberg Colloquium on Glassy dynamics and Optimization. Springer, Heidelberg 1366
39. de Simone C, Diehl M, Jünger M, Mutzel P, Reinelt G, Rinaldi G (1995) J Stat Phys 80:487 **TSS** 1368
40. Lawler EL (1976) Combinatorial optimization: Networks and matroids. Holt, Rinehart and Winston, New York 1369
41. Derigs U (1988) Programming in networks and graphs. Lect Note Econ Math Syst 300 **CE6** 1370
42. Barahona F (1982) J Phys A 15:3241; Barahona F, Maynard R, Rammal R, Uhry JP (1982) J Phys A 15:673 **TSS** 1371
43. Kawashima N, Rieger H (1997) Europhys Lett 39:85 **TSS** 1372
44. Hartmann AK, Young AP (2002) Phys Rev B 66:094419; Hartmann AK, Bray AJ, Carter AC, Moore MA, Young AP (2002) Phys Rev B 66:224401 **TSS** 1373
45. Amoroso C, Hartmann AK, Hastings MB, Moore MA (2006) Phys Rev Lett 97:267202; Bernard D, LeDoussal P, Middleton AA (2007) Phys Rev B 76:020403(R) **TSS** 1374
46. Cardy J (2005) Ann Phys 318:81; Bauer M, Bernard D (2006) Phys Rep 432:115 **TSS** 1375
47. Liers F, Jünger M, Reinelt G, Rinaldi G (2004) In: Hartmann A, Rieger H (eds) New optimization algorithms in physics. Wiley, Berlin 1376
48. Chvátal V (1983) Linear programming. Freeman, San Francisco 1377
49. Grötschel M, Lovász L, Schrijver A (1988) Geometric algorithms and combinatorial optimization. Springer, Berlin, Heidelberg 1378
50. Wu FY (1982) The Potts Model. Rev Mod Phys 54:235 1379
51. Kasteleyn PW, Fortuin CM (1969) J Phys Soc Jpn 46:11 **TSS** 1380
52. Juhász R, Rieger H, Iglói F (2001) Phys Rev E 64:056122 **TSS** 1381
53. Schrijver A (2003) Combinatorial Optimization – Polyhedra and Efficiency, vol B. Springer, Berlin 1382
54. Grötschel M, Lovász L, Schrijver A (1981) Comb 1:169 **TSS** 1383
55. Iwata S, Fleischer L, Fujishige S (2001) J ACM 48(4):761 **TSS** 1384
56. Schrijver A (2000) J Comb Theory Ser B 80:346 **TSS** 1385
57. Edmonds J (1977) In: Guy R, Hannani H, Sauer N, Schönheim J (eds) Combinatorial Structures and Their Applications. Gordon and Breach **CE7** 1386
58. Kasteleyn PW, Fortuin CM (1969) Phase transitions in lattice systems with random local properties. J Phys Soc Jpn 26:11 1387
59. Anglés d'Auriac JC, Iglói F, Preissmann M, Sebö A (2002) J Phys A 35:6973 **TSS** 1388
60. Anglés d'Auriac JC (2004) In: Hartmann A, Rieger H (eds) New optimization algorithms in physics. Wiley, Berlin 1389
61. Anglés d'Auriac JC, Iglói F (2003) Phys Rev Lett 90:190601; Mercaldo MT, Anglés d'Auriac J-C, Iglói F (2004) Phys Rev E 69:056112; Mercaldo MT, Anglés d'Auriac J-C, Iglói F (2005) Europhys Lett 70:733 **TSS** 1390
62. Fisher DS (1992) Phys Rev Lett 69:534; (1995) Phys Rev B 51:6411 **TSS** 1391
63. Zeng C, Middleton AA, Shapir Y (1996) Phys Rev Lett 77:3204 **TSS** 1392
64. Middleton AA (1999) Phys Rev Lett 83:1672 **TSS** 1393
65. Anglés d'Auriac J-C, Sourlas N (1997) Europhys Lett 39:473 **TSS** 1394
66. Anglés d'Auriac J-C, Preissmann M, Sebö A (1997) Math Comput Model 26:1 **TSS** 1395
67. Pal KF (2004) In: Hartmann A, Rieger H (eds) New optimization algorithms in physics. Wiley, Berlin 1396
68. Boettcher S (2004) In: Hartmann A, Rieger H (eds) New optimization algorithms in physics. Wiley, Berlin 1397
69. Weigt M (2004) In: Hartmann A, Rieger H (eds) New optimization algorithms in physics. Wiley, Berlin; Cocco S, Ein-Dor L, Monasson R (ibid); Zecchina R (ibid) 1398
- Books and Reviews 1428
- Alava M, Duxbury P, Moukarzel C, Rieger H (2000) Combinatorial optimization and disordered systems. In: Domb C, Lebowitz JL (eds) Phase Transition and Critical Phenomena, vol 18. Academic Press, Cambridge 1429
- Hartmann A, Rieger H (2002) Optimization Algorithms in Physics. Wiley VCH, Berlin 1430
- Hartmann A, Rieger H (2004) New Optimization Algorithms in Physics. Wiley VCH, Berlin 1431
- Hartmann AK, Weigt M (2005) Phase Transitions in Combinatorial Optimization Problems. Wiley-VCH, Berlin 1432

CE6 Please add page numbers.

CE7 Please add publisher location.